Journal of the European Ceramic Society 21 (2001) 2229–2241
www.elsevier.com/locate/jeurceramsoc

Tetragonal-to-monoclinic phase transformation in CeO_2-stabilised zirconia under uniaxial loading

G. Rauchs [a,1], T. Fett [b,*], D. Munz [a, b], R. Oberacker [c]

[a] *Universität Karlsruhe, Institut für Zuverlässigkeit und Schadenskunde im Maschinenbau, D-76021 Karlsruhe, Germany*
[b] *Forschungszentrum Karlsruhe, Institut für Materialforschung II, D-76021 Karlsruhe, Germany*
[c] *Universität Karlsruhe, Institut für Keramik im Maschinenbau-Zentrallabor, Haid und Neustr. 7, D-76131 Karlsruhe, Germany*

Received 27 November 1999; received in revised form 22 August 2000; accepted 31 August 2000

Abstract

The critical transformation stresses of five 9 mol% Ce-TZP materials with different grain sizes have been investigated in bending. It was found that two different types of phase transformation mechanisms occur in these materials. (a) A homogeneous phase transformation with a transformation strain increasing continuously with increasing applied stress. This transformation type produces the initial deviation from linear–elastic material behaviour in the stress–strain curves. (b) An autocatalytic phase transformation with the autocatalytic formation of transformation bands, leading to a strongly inhomogeneous, localised distribution of the monoclinic phase. Their locations and sizes vary randomly. The formation of the transformation bands has been monitored by acoustic emission recording. The amount of monoclinic phase content has been quantified by X-ray diffractometry and Raman spectroscopy.

Keywords: CeO_2; Grain size; Mechanical properties; Phase transformation; ZrO_2

1. Introduction

Stabilised zirconia ceramics undergo a stress-induced tetragonal-to-monoclinic phase transformation which produces a strong *R*-curve behaviour and high fracture toughnesses. From this point of view, ceria-stabilized zirconia, which show a large amount of phase transformation and a strong transformation potential, lead to the prospect of a flaw-tolerant ceramic material for structural applications. Nevertheless, prior to any practical applications, further research has to be performed in order to improve the understanding of the transformation behaviour of this class of materials with respect to the stress level required to trigger the phase transformation and the plastic transformation strains involved in that process. Additionally, the effect of grain size, which is a key parameter for the production of a ceramic material, on phase transformation has to be elucidated.

The metastable, tetragonal phase may turn into the monoclinic lattice structure in an athermal, diffusionless process. In the absence of stresses transformation takes place by cooling below the so-called martensitic start temperature M_s. The phase transformation can also be triggered by mechanical loading. It is well known that temperature influences the stresses required to trigger transformation, i.e. the required stresses increase with increasing temperature.

The tetragonal phase shows a strong thermal expansion anisotropy, influenced by the type and concentration of the stabilising cations. After sintering, the thermal anisotropy induces eigenstresses σ_{TEA} which depend on the grain size d, the difference of the thermal expansion coefficients $\Delta\alpha_{th}$ in a- and c-direction, the temperature difference ΔT and the distance r from the grain boundary triple points[1]

$$\sigma_{TEA} \propto \Delta\alpha_{th}\Delta T\frac{d}{r}. \quad (1)$$

Since the eigenstresses are proportional to the grain size, the external stresses needed to trigger the phase transformation decrease with increasing grain size. On the other hand, grains smaller than a critical size cannot

* Corresponding author.
E-mail address: theo.fctt@imf.fzk.de (T. Fett).
[1] Present address: Manchester Materials Science Centre, University of Manchester, Grosvenor Street, Manchester M1 7HS, UK

0955-2219/01/$ - see front matter
PII: S0955-2219(00)00258-2

undergo the phase transformation due to the lack of nucleating defects. It can be concluded that grain size has a crucial influence on the stresses required to induce the phase transformation.

Through the lattice parameters of both phases, a volume dilatation of 4.5% and shear strains of 16% can be attributed to the tetragonal-to-monoclinic phase transformation.[2] Different combinations of the lattice axes lead to several transformation variants. The transformation shear strains are strongly reduced by twinning.[2,3] In many cases this has led to the assumption that the shear strains can be neglected. The transformation strains of the different transformation variants differ by a small amount, which, after averaging over a large number of transformed grains[4] and neglecting the shear strains, leads to an isotropic plastic transformation strain. This simplified approach which is frequently used in theoretical considerations[5] has been refuted in strain and texture investigations.[6]

In partially stabilised zirconia, transformable tetragonal particles totally transform to the monoclinic phase, with the orientation of the lattice cells being prescribed by the orientation axes of the ellipsoidal parent particle.[3] In TZP ceramics, the transformation is not complete, neither in the transforming grains nor over macroscopic regions,[7] thus causing a remaining tetragonal phase content after transformation. Parts of a grain or full grains, which are below a critical size or whose load is reduced by neighbouring transformed grains, remain in the tetragonal phase. In cooling experiments, a small amount of transformation strain, which continuously increases with decreasing temperature, has been observed after the martensitic burst[1] and attributed to the transformation of a part of the microscopic regions which did not transform during the martensitic burst due to their morphology.

The transformation of a grain produces high strains which can trigger the phase transformation in adjacent grains. Thus, macroscopic regions can transform in a burst-like event into the monoclinic phase. This effect has been observed in experiments as transformation bands on uncracked specimens[8–12] and as crack tip transformation zones.[9,13–15] The martensitic burst during cooling is attributed to the same effect. This autocatalytic phase transformation is limited to zirconia ceramics with a high transformation potential. Band-like transformation structures have also been found in MgO-PSZ: so-called shear bands are formed during the twinning of the transformed monoclinic phase. They are limited to the grain size of the non-transformable cubic matrix of these materials.[16] Therefore, the extension of the shear bands in PSZ is by approximately two orders of magnitude smaller than that of transformation bands in TZP.

There is experimental evidence that the mechanically induced phase transformation is not irreversible, with an isothermal backtransformation taking place upon unloading or compressive loading.[17,18] Unloading Vickers indents by cutting them free leads to a decrease of the surface roughness, which is typical for phase transformation.[19] Whereas autocatalytically transformed domains are believed to be irreversible, subcritically transformed regions may partially retransform to the tetragonal parent phase. In cyclic loading of MgO-PSZ, a hysteresis of the plastic transformation strains was found, with the contribution of backtransformation and microcrack closure being reflected by the specific curvature of the hysteresis curve.[20] A decrease of the transformation strains during unloading was also found in Y-TZP.[21,22]

In this paper, the transformation behaviour of 9 mol% Ce-TZP with five different grain sizes is investigated under bending loading to assess the influence of grain size on the critical stress levels required to trigger the phase transformation, on the plastic transformation strains and on the morphology of the transformed material.

2. Experimental procedures

2.1. Specimen preparation

The test materials were prepared from a batch of 9 mol% CeO_2–ZrO_2 powder (Unitec PCE 14.0–002 s). The processing parameters of previous studies[10,23,24] have been used: after die pressing at 10 MPa, the plates were isostatically repressed at 200 MPa. The green plates were sintered in air at variable temperatures ranging from 1400 to 1600°C, with heating and cooling rates of 3°C/min. In Table 1 the different materials are named CeI to CeV. The mechanical test specimens were prepared from the sintered plates by diamond cutting and grinding. One specific specimen surface was polished with diamond paste of a grain size down to 1 μm. The specimens were annealed in air at 1200°C for 2 h in order to revert the monoclinic phase produced during machining to the tetragonal symmetry and to reduce the machining-induced residual stresses. The specimen density was determined by the Archimedes method. Grain size was investigated using SEM pictures according to the line-intercept method.

2.2. Investigation of the monoclinic phase content

Phase content evaluation on the macroscopic scale has been performed using an X-ray diffractometer with CuK_α radiation. The monoclinic phase content was determined through the integral intensities of the tetragonal (111), monoclinic (111) and (11-1) peaks according to Ref. 25.

Local phase evaluation has been conducted using a Raman spectroscope in conjunction with a microscope. This allows a fast phase analysis with a minimum spot

Table 1
Properties of the five materials

Material	Sintering temperature (°C)	Grain size (μm)	Young's modulus (GPa)	Density (%)	$c_{m,0}$ (%)	σ_c (MPa)	σ_{AE} (MPa)
CeI	1400	0.9	188	97.6	6.2	156	
CeII	1450	1.4	197	99.9	2.0	210	336
CeIII	1500	1.7	199	99.9	2.1	240	320
CeIV	1550	2.1	198	99.8	2.1	282	312
CeV	1600	2.5	197	99.6	1.9	301	294

size of 1 μm.[26,27] The Raman spectrum was fitted with Lorentzian peaks using an arbitrarily fixed background. The phase content evaluation was based on the integral intensities of the tetragonal and monoclinic peaks at 143 and 257 and at 171 and 183 cm^{-1}, respectively.

The monoclinic phase content can be calculated as the ratio of the integral intensities:[28]

$$c'_m = \frac{I_m}{I_m + I_t} = \frac{I_m^{171} + I_m^{186}}{I_m^{171} + I_m^{186} + I_t^{143} + I_t^{257}}. \quad (2)$$

The results of Eq. (2) were far smaller than the monoclinic phase content measured by XRD. In fact, Eq. (2) has been developed for the phase content evaluation of MgO-PSZ which has a monoclinic phase content between 10 and 40%. In Ce-TZP, the monoclinic phase content ranges from 0 to 80%. The lower values are caused by the strongly differing width of the Raman peaks, i.e. especially by the broad tetragonal peak at 257 cm^{-1}, which yields high integral intensities at very low monoclinic phase contents and therefore strongly influences the results.

Assuming that the integral intensities are proportional to the monoclinic phase content, a corrected monoclinic phase content c_m can be calculated:[29]

$$c_m = \frac{Q \cdot c'_m}{1 + (Q-1)c'_m}. \quad (3)$$

The constant $Q = 2.4$ was evaluated using results from X-ray diffractometry. Raman measurements have been made on two different scales:

- Macroscopic line scans along the stress gradient of the specimens with a step size between 2 and 4 mm, a counting time of 300 s and a spot size of 38 μm to monitor the relationship between the applied stress and the monoclinic phase content.
- Line scans perpendicular to transformation bands, with a step size of 5 μm, a counting time of 150 s and a spot size of 7 μm to evaluate the local monoclinic phase content in transformation bands. A spot size of 7 μm was used instead of the maximum resolution of 1 μm to obtain a monoclinic phase content averaged over several grains.

2.3. Cooling experiments

Using a cryostatic device, zirconia specimens have been cooled down gradually to −80°C in silicon oil. The temperature has been recorded using thermocouples. The strain of the specimens has been recorded either by using strain gauges or by LVDTs. Due to high straining during the autocatalytic burst, no strain data were available after the occurrence of the burst. The transformation strains have been estimated roughly by comparing the geometry of the specimen before and after the experiment. After the cooling experiment, the monoclinic phase content was investigated by X-ray diffractometry.

2.4. Mechanical experiments

A specimen geometry of 4×3×48 mm^3 and roller spacings of 40 and 20 mm was used for the four-point bend tests, with the following parameters being recorded during testing:

- The load F with a load cell to assess the applied stress.
- The local strain at the location of the maximum stress with strain gauges. On some four-point bending specimens, both the longitudinal and the transverse strains have been recorded.
- The acoustic emission with a piezosensor having a resonance frequency of 150 kHz and a low-pass filter of 100 kHz. The device was fixed on the load frame or specimen holders. Coupling of the piezosensor to the structure was achieved by applying silicon glue. The acoustic emission signal enabled the monitoring of the formation of autocatalytic transformation bands.

The Young's modulus and Poisson's ratio were determined from stress–strain curves. The applied stresses have been calculated from the applied load F. The slope of the linear–elastic part of the stress–strain curves was determined by linear regression. The combination of the stress–strain curves with the acoustic emission signal the monitoring of the onset of phase transformation with two different methods:

- At the intersection of the stress–strain curve with a line parallel to the elastic load line, shifted 5 ppm

to the right, the onset of plastic deformation could be monitored. The stress at the intersection point provides the critical stress σ_c.

- The onset of autocatalytic transformation band formation, producing audible noise and strong acoustic emission signals at the critical stress σ_{AE}.

After mechanical testing, the monoclinic phase content was investigated on a macroscopic scale using XRD and on a microscopic scale using Raman spectroscopy. The geometry of the autocatalytic transformation bands was monitored under a microscope.

3. Results

3.1. Material characterisation

The as-delivered zirconia powder had a specific surface of 1.6 m^2/g and a mean particle size of 0.7 μm. After sintering, the materials CeII through CeV had a density of more than 99% of theoretical density. CeI had a slightly lower density of 97.6%. Post-densification of this material by hot isostatic pressing resulted in strongly cracked and damaged plates. It has to be presumed that CeO_2 is reduced to Ce_2O_3 at high temperatures in a low-oxygen atmosphere,[30] which detrimentally affects the stability of the tetragonal phase.[31]

The monoclinic phase content of the plates after various processing steps was evaluated by XRD. After grinding, a high monoclinic phase content between 20 and 30% was found. This monoclinic phase is confined to a region of several micrometres at the surface, since Raman spectroscopy with its higher penetration depth showed no significant monoclinic phase content at all after grinding.

Polished surfaces exhibited far lower monoclinic phase contents. After annealing at 1200°C, the monoclinic phase produced by machining was nearly totally reduced, thus resulting in an initial monoclinic phase content $c_{m,0}$ of approx. 2%. No difference of the monoclinic phase content in polished and ground surfaces was visible after annealing. Therefore, experiments could be performed with nearly fully tetragonal materials. Only CeI had a monoclinic phase content of 6% after annealing. A shift of the intensity of the (200) and (002) XRD peaks was monitored on polished surfaces. This indicates texture formation during polishing.

The Young's modulus of CeI was slightly lower than that of the other materials. This is due to the lower density of this material. During mechanical testing, a Poisson's ratio of 0.30 was found for all materials. The most important material parameters of the five materials investigated are shown in Table 1.

The grain size was determined using SEM pictures. A mean grain size ranging from 0.9 to 2.5 μm was achieved by varying the sintering temperature. Fig. 1(a) shows that in CeI a large number of smaller grains exists along with some larger grains. This may be considered a bimodal grain size distribution. The other materials exhibited precipitates on the surface after annealing [Fig. 1(b)]. Based on BSE pictures, it was found that these precipitates have a lower zirconium content than the bulk material. The small size of the precipitates inhibited the use of EDX for assessing the exact composition.

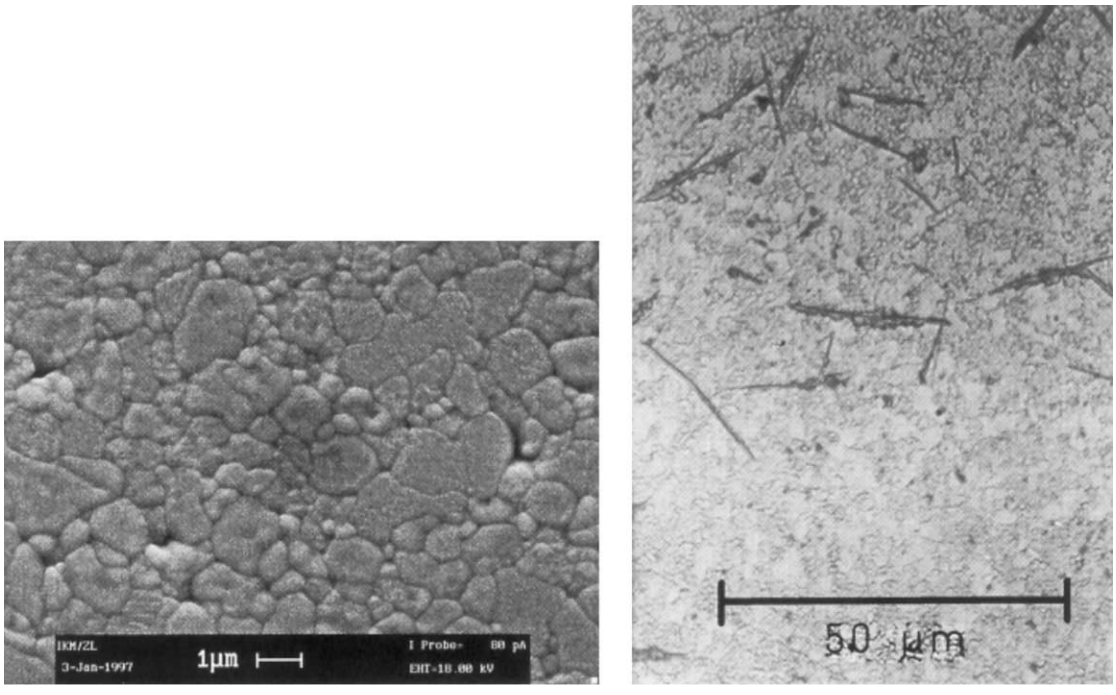

Fig. 1. (a) SEM micrograph of CeI; (b) micrograph of surface precipitates.

3.2. Cooling experiments

During cooling of the specimens in silicon oil down to −80°C, a tetragonal-to-monoclinic phase transformation was observed. In CeI, having a grain size of 0.9 μm, a continuous increase of transformation strain was observed, starting from −70°C (Fig. 2). No martensitic burst was observed in this temperature range. Its occurrence cannot be excluded for lower temperatures. In the materials with larger grain size, a martensitic burst with a spontaneous increase of the transformation strain was observed at temperatures between −68 and −57°C (Fig. 2). Despite the strong scatter in the martensite start temperature, a slight increase of the martensite start temperature with increasing grain size can be identified (Fig. 3).

Due to the sudden jump in strain during the martensitic burst, the strain gauges were damaged, which inhibited the measurement of strains after the martensitic transformation. Therefore, the strains caused by the martensitic burst had to be evaluated by measuring the geometry of the specimen before and after the experiment. A linear transformation strain of 1.3% was found for CeII through CeV. CeI shows only a small amount of transformation strain, which is in accordance with the missing autocatalytic burst.

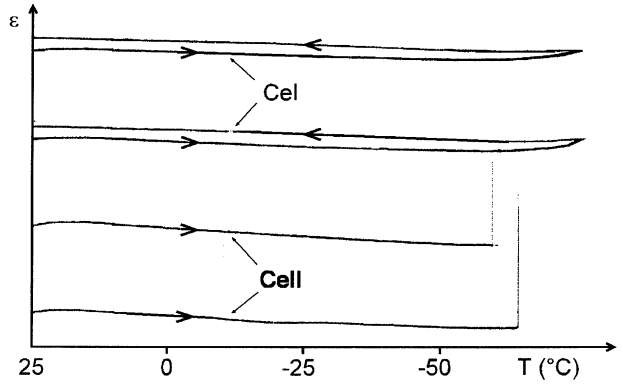

Fig. 2. Temperature–strain diagram of two specimens of CeI and CeII.

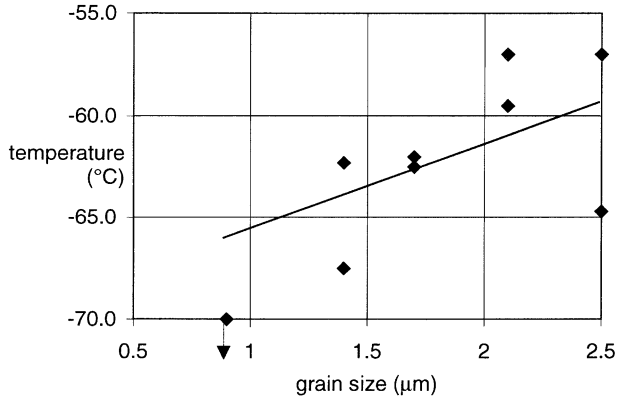

Fig. 3. Influence of the grain size on the martensite start temperature.

X-ray diffractometric phase evaluation after the experiments revealed an additional monoclinic phase content of approx. 4% in CeI. For CeII through CeV, the increase of the monoclinic phase content was found to be independent of the grain size. On ground surfaces, a monoclinic phase content of about 75% was detected, which corresponds to the values derived from the volume change. On polished surfaces, a monoclinic phase content of 55% was found. A comparison of the integral intensities of the (200)- and (002) peaks showed a texture of the polished surface, which remained unchanged by the martensitic burst. It has to be presumed that this texture is a surface effect occurring during polishing of the surface.

After cooling some CeI specimens in liquid nitrogen, a volume dilatation of 0.8%, which corresponds to an increase of the monoclinic phase content of 53%, was observed. It could not be determined, whether a martensitic burst did happen or whether the phase transformation took place in a continuous way. The cooling experiments showed that CeI with a continuous increase of the transformation strains during cooling exhibits a different material behaviour than the other materials examined.

The violent martensitic burst is accompanied by audible noise. The sudden increase in transformation strains strongly damages the specimen. In fact, the specimens exhibited a large number of macroscopic cracks after the martensitic burst, with some specimens fragmenting during the martensitic burst.

3.3. Phase transformation during mechanical loading

During the loading experiments, a tetragonal-to-monoclinic phase transformation was observed. The phase transformation was monitored by stress–strain curves and by acoustic emission. Fig. 4 shows the stress–strain curves of four-point bending experiments for the materials CeI and CeII, with an initial linear–elastic regime, followed by elastic–plastic deformation arising from the tetragonal-to-monoclinic phase transformation. A saturation of the phase transformation with a subsequent linear–elastic material response has not been observed. Such a material behaviour is not to be expected due to the inhomogeneous stress field in bending, in contrast to the homogeneous stress field in pure tension. Acoustic emission signals produced by the burst-like formation of autocatalytic transformation bands are monitored from a critical stress level on [Fig. 4(b)]. Materials CeIII, CeIV and CeV showed a behaviour similar to that of material CeII, shown in Fig. 4(b). Acoustic emission signals have been received until fracture or load reversal. No acoustic emission signals have been monitored during unloading. In sub-

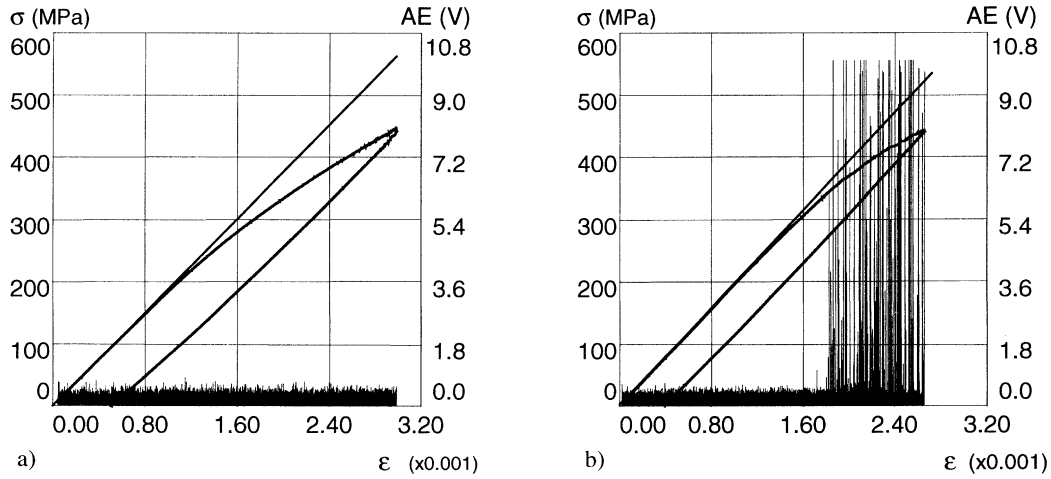

Fig. 4. Stress–strain curve with acoustic emission signals in four-point bending of (a) CeI; (b) CeII.

sequent load cycles, autocatalytic transformation sets in at the maximum stress reached by the previous load cycle. The critical principal stresses for the onset of homogeneous and autocatalytic phase transformation are presented in Table 1.

The stress–strain curves show that the formation of autocatalytic transformation bands does not coincide with the onset of non-linear material behaviour. Therefore, a systematic distinction is made between the critical stress σ_c which is related to the onset of non-linear material behaviour due to phase transformation, on the one hand, and the critical stress σ_{AE} related to the onset of autocatalytic transformation band formation.

Despite the large transformation strains recorded in CeI, no autocatalytic transformation band formation was detected in this material, either by acoustic emission or by microscopical observation.

Fig. 5 shows the influence of grain size on the two critical transformation stresses. The critical stresses for autocatalytic transformation decrease from 340 to 300 MPa with increasing grain size. It should be noticed that the decrease of the transformation stress is small. The critical stresses, at which the homogeneous phase transformation sets in, are increasing from 160 to 300 MPa with increasing grain size. For grain sizes <2.5 μm these critical stresses are below the critical stresses of the autocatalytic phase transformation, i.e. the homogeneous transformation sets in before the occurrence of autocatalytic transformation. The difference between the two critical stresses decreases strongly with increasing grain size, with the stresses being nearly equal in CeV. A further homogeneous transformation after the beginning of autocatalytic phase transformation is possible, but cannot be monitored in the stress–strain curves. It is possible that in CeV homogeneous phase transformation sets in after autocatalytic phase transformation, but in the stress–strain curve no critical

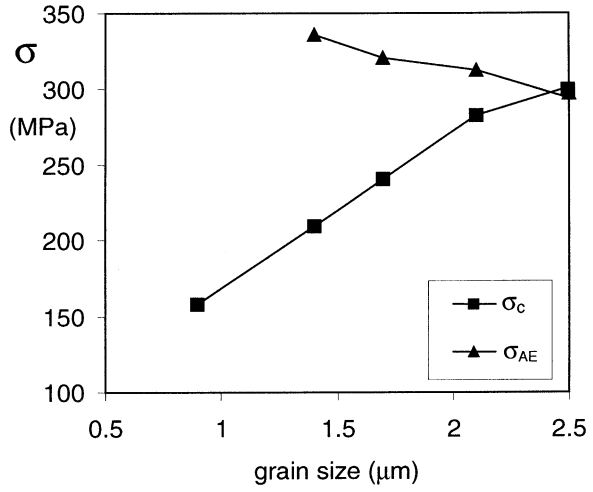

Fig. 5. Critical stresses for homogeneous and for autocatalytic transformation vs grain size.

homogeneous stress can be determined after the onset of autocatalytic phase transformation.

The grain size has an opposite effect on the two phase transformation stresses. The different grain size dependencies show that homogeneous and autocatalytic phase transformations are to be considered two different transformation mechanisms. A comparison of the transformation behaviour of the different materials shows that in CeI homogeneous transformation takes place only, whereas in CeV the main transformation mechanism is autocatalytic phase transformation. In the materials CeII, CeIII and CeIV, both transformation mechanisms take place.

3.4. Plastic strains

Fig. 6(a) and (b) show the plastic strains of CeI and CeIII. In these diagrams, the influence of the plastic

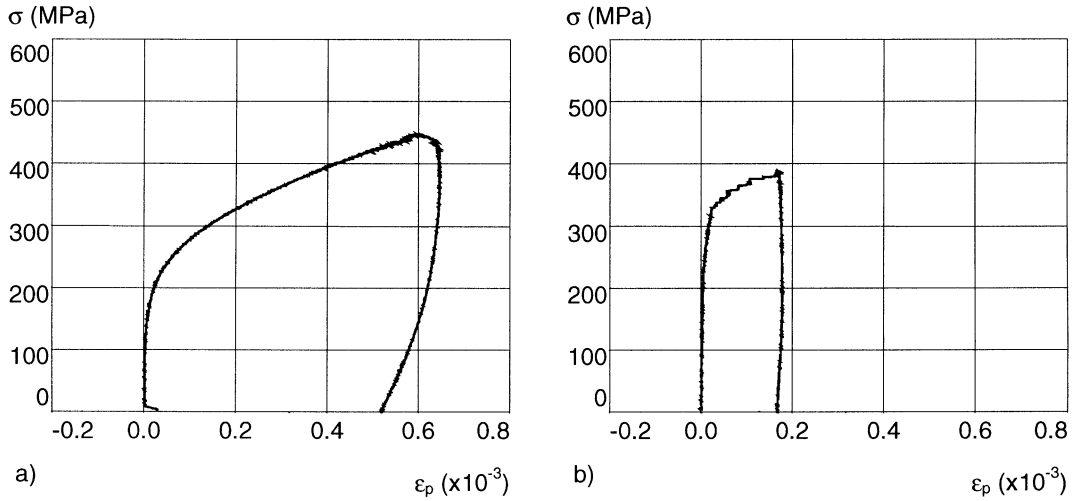

Fig. 6. Stress–plastic strain curve of four-point bending experiments: (a) CeI; (b) CeIII.

strains on the outer fibre stress has been neglected, i.e. the stresses have been calculated using the load and the specimen geometry, assuming a linear stress distribution. The curves of CeII, CeIV and CeV look similar to those of material CeIII. The curves show that the burst-like formation of transformation band leads to small steps in the plastic strain. An acoustic emission peak can be attributed to each step-like strain increase. The discontinuous formation of a transformation bands below the strain gauge leads to discontinuous strain steps. The amount of homogeneous plastic strain before the onset of autocatalytic band formation strongly decreases with increasing grain size.

Due to the absence of autocatalytic transformation and the homogeneous distribution of the transformation strains in CeI, the influence of the transformation strains on the bending stress stress distribution in the specimen during loading could be calculated using an iterative computing scheme of Ref. 32. Using the stress–strain curve [Fig. 6(a)], the true stress was calculated for different load levels, which enabled the calculation of the true plastic strains from the total strains measured. This corrected stress–strain curve was introduced again in the computing scheme. This process was repeated iteratively until convergence of the stress–strain curve. The resulting stress–strain curve (Fig. 7) is equivalent to stress–strain curves which would be measured in pure tension. Compared to the linear stress distribution calculated from the applied load and the specimen geometry, the true stresses at the bending specimen's surface are approx. 25% lower. The plastic strains calculated by this method are nearly twice as high as the strains calculated using a linear stress distribution. It has to be concluded that the plastic transformation strains have a high impact on the stress distribution in bending specimens, which has to be accounted for in the case of bending strength measurements. This explains

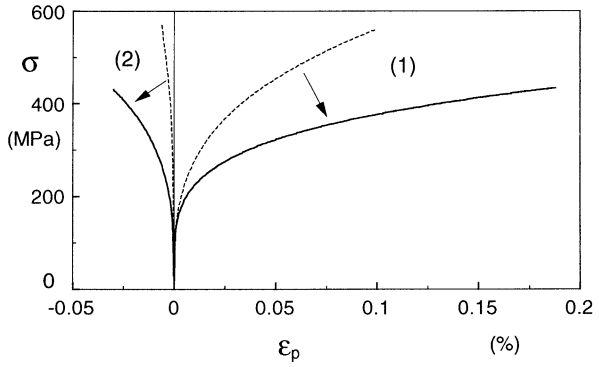

Fig. 7. Longitudinal (1) and transverse (2) plastic strains in four-point bending; dashed curves: uncorrected data, solid curves corrected according to Ref. 32.

why the strength measured in four-point bending is higher than that measured in pure tension.

An increase of the monoclinic phase content of 5 and 7% was found in CeI specimens by X-ray diffractometry after loading to 330 and 560 MPa in four-point bending. From this monoclinic phase content, the corresponding plastic strain can be calculated under the assumption of isotropic volume dilatation. The amount of plastic strains approaches the values of the plastic strains determined from the stress–strain curve with the effects of plastic strain on the stress field being included. On the compressive side of the bending specimen, no increase of the monoclinic phase content was found. It has to be concluded that the high critical stresses needed to induce the phase transformation under compressive stresses[11,16,33–35] cannot be reached in bending experiments due to the early fracture caused by the tensile stresses.

In the other materials, no increase of the monoclinic phase content was found using X-ray diffractometry after loading. On the one hand, this may be caused by

the small amounts of homogeneous transformation strains, which lie below the resolution of X-ray diffractometry. On the other hand, due to the low spatial resolution, an average value between the monoclinic phase content of the transformation bands and the nearly fully tetragonal background is measured, with the influence of the transformation bands vanishing because of their small surface fraction. This implies that the phase composition of the transformation bands cannot be analysed using X-ray diffractometry.

In CeI, which shows the highest plastic strains, the measured difference of the ratio of tetragonal (200)- and (002) intensities before and after loading did not exceed the resolution of the analytical method. Taking into consideration predictions from Ref. 36 that a ferroelastic domain switching yields plastic strain of 0.2% should lead to a substantial increase of the ratio of the tetragonal (200)- and (002) peaks from 2 to 5, it is obvious that no texture formation, i.e. ferroelastic domain switching, occurred during mechanical loading.

On CeI, the monoclinic phase content depends on the applied stress, with the maximum monoclinic concentration in the maximally stressed specimen centre, decreasing towards the unstressed edge of the specimen. In contrast to the autocatalytic phase transformation, the homogeneous phase transformation follows a subcritical pattern, i.e. the monoclinic concentration depends on the applied stress.

Fig. 6 shows a decrease of the plastic strains during unloading. Due to the convex shape of the curve, microcrack closure has to be discarded as an explanation for this material behaviour,[20] and therefore, it has to be assumed that a monoclinic-to-tetragonal backtransformation is taking place. The amount of backtransformation strongly decreases with increasing grain size. This grain size dependence as well as the fact that during unloading no acoustic emission signals were monitored leads to the conclusion that a part of the homogeneously transformed tetragonal phase is affected by backtransformation. Similar results concerning backtransformation were found in Ref. 19.

Fig. 7 shows the stress vs plastic strain curves with and without the influence of the transformation strains on the stress field. It becomes obvious that the transverse plastic strains are much smaller than the longitudinal plastic strains. Using a strain gauge rosette, it was experimentally shown that the principal axes of the plastic strains coincide with the longitudinal and transverse direction of the bending specimen.

3.5. Autocatalytic transformation structures

On the specimen surfaces of the materials CeII through CeV, a large number of autocatalytic transformation bands is created during loading. A microscopic image of transformation bands is shown in Fig. 8.

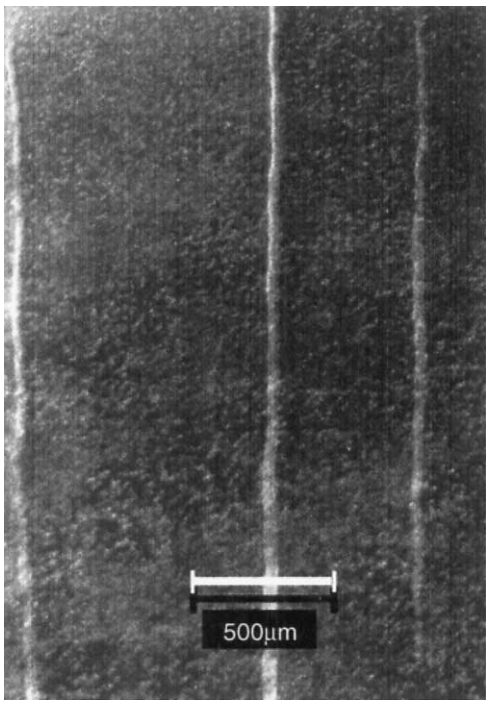

Fig. 8. Autocatalytic transformation bands at the tensile surface of a four-point bending specimen (CeII).

The transformation bands have a variable width between 20 and 100 μm and are irregularly spaced. In uniaxial bending, the transformation bands are oriented parallel to each other, stretching in the transverse direction of the specimen. On bending surfaces under compressive loads, no autocatalytic transformation bands have been found, which leads to the conclusion that in the investigated stress range autocatalytic transformation occurs under tensile loads only.

In the macroscopic Raman-spectroscopic line scans over the specimens, no increase of the monoclinic phase content was found in CeII through CeV. The small amount of monoclinic phase outside of the transformation bands caused by homogeneous phase transformation is below the resolution limit of Raman spectroscopy, thus making it impossible to detect any significant variation of the monoclinic phase content with the applied stress. The monoclinic phase content of autocatalytic transformation bands was monitored by microscale Raman-spectroscopic line scans. No increase of the monoclinic phase content was detected outside of the transformation bands in CeII through CeV. The monoclinic phase is localised in the transformation bands. Fig. 9 shows the monoclinic concentration of line scans perpendicular to transformation bands. The change of the monoclinic phase content across the edges of the bands is steep with a nearly constant concentration inside of the bands, which shows that the autocatalytic phase transformation follows a supercritical transformation pattern. The scatter of the data inside the transformation band results from the measuring

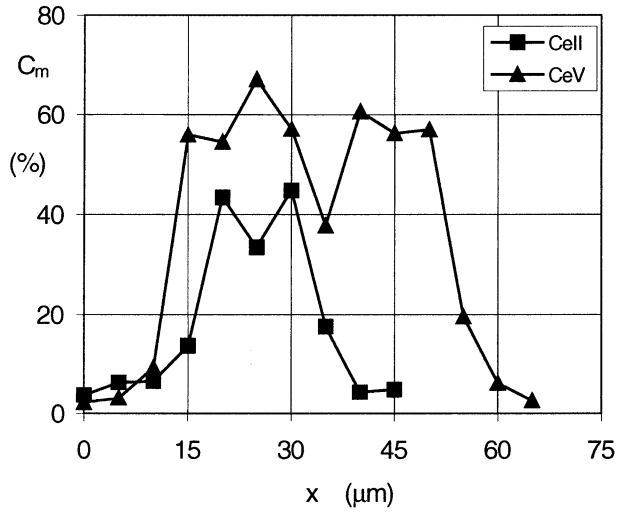

Fig. 9. Monoclinic phase content perpendicular to individual transformation bands in CeII and CeV.

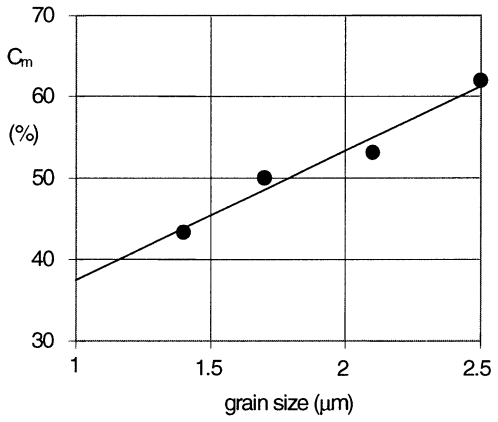

Fig. 10. Monoclinic concentration of the autocatalytic transformation bands as a function of grain size.

spot size of 7 μm, which leads to an averaging process over a small number of grains.

The maximum amount of monoclinic phase in autocatalytic transformation bands was 75%. Fig. 10 shows the average plateau value of the monoclinic phase content inside the transformation bands. This value increases with increasing grain size. In narrow transformation bands, low monoclinic concentrations have been found. This is a result of the averaging attributed to the laser spot size of 7 μm.

4. Discussion

During the mechanical experiments of Section 3.3, it was found that the onset of autocatalytic transformation band formation, monitored by acoustic emission, does not coincide with the onset of plastic deformation. In fact, a continuously increasing plastic strain was monitored before the onset of autocatalytic phase transformation in all materials investigated in this study. This has lead to the distinction between two characteristic stresses: on the one hand, σ_c which is defined by the onset of non-linear deformation and, on the other hand, σ_{AE} defined by the onset of autocatalytic transformation band formation. Thus, a clear distinction between two types of phase transformation events is made:

- Homogeneous phase transformation producing a continuously increasing transformation strain with increasing applied load characterised by the critical stress σ_c.
- Autocatalytic phase transformation with a burst-like formation of transformation bands characterised by the critical stress σ_{AE}.

The suitability of that subdivision is further backed by the opposing trends of the grain size influence on the critical transformation stresses. The grain size has a strong influence on the critical stresses of the homogeneous phase transformation. The critical stress of the homogeneous phase transformation, σ_c, increases strongly with increasing grain size. For the autocatalytic transformation observed in materials CeII through CeV, the critical stresses show a slight decrease with increasing grain size. This is due to eigenstresses resulting from thermal expansion anisotropy and increasing with increasing grain size. Similar grain size dependencies for the autocatalytic phase transformation have been reported for other ceria-stabilised zirconia in Refs. 8,10,11,14. The results from Section 3.2 show a slight increase of the martensite start temperature with increasing grain size. The small variation of the martensite start temperature compared to results from Ref. 1 can be explained by the fact that those results rely on investigations of 12Ce-TZP, where the variation of the grain size from 1.3 to 8 μm was much higher than in our investigation on 9Ce-TZP, where the achievable grain size range is much smaller. In the materials CeII through CeV, both transformation types have been observed.

The results of Sections 3.3 and 3.4 point to the existence of plastic deformation in CeI, the amount of which is continuously increasing with increasing load or decreasing temperature. The continuous increase of the plastic strains with the applied stress can be explained by the fact individual tetragonal grains require different applied stresses to transform, depending on their size and orientation. A similar transformation behaviour has been described in Refs. 18,20,34,37 and Ref. 21 for MgO-PSZ and Y-TZP respectively. Those materials are characterised by the small size of the transformable tetragonal entities — particles in the case of MgO-PSZ and matrix grains for Y-TZP, which was in some cases below 1 μm. This leads to the conclusion that CeI, due to its small grain size which is comparable to that of some Y-TZP materials, shows a similar transformation

behaviour. In Section 3.5, the homogeneous plastic deformation has been identified as transformation-induced plasticity by X-ray diffractometry and Raman spectroscopy. A texture formation in the tetragonal phase due to ferroelastic domain switching has not been found in X-ray diffractometric investigations after mechanical loading or cooling. It has to be concluded that, in contradiction to other investigations,[21,36] no ferroelastic domain switching occurred at the investigated load levels and that hence the plasticity in CeI is produced by the phase transformation only.

The amount of homogeneous transformation strains produced during loading strongly decreases with increasing grain size to a very low level. This is probably caused by the grain size distribution. Assuming that only grains below a critical size can contribute to the homogeneous phase transformation and considering that the number of those grains diminishes with increasing average grain size, the amount of homogeneous transformation strains has to decrease with increasing grain size. In CeII through CeV, autocatalytic phase transformation has to be considered the main transformation mechanism in these materials. In CeII through CeV, no monoclinic phase content could be traced experimentally outside of the transformation bands. This implies that the autocatalytic phase transformation follows a supercritical transformation scheme, i.e. the monoclinic phase content of the transformation structures jumps to a nearly constant value during transformation.

It was found that the homogeneous transformation strains depend on the orientation of the applied load: the transverse transformation strains were considerably smaller in magnitude than the transformation strains parallel to the applied stress and were opposite in sign, i.e. the phase transformation produces a plastic contraction in transverse direction. Similar results have been found in compression experiments.[11,16] It has to be assumed that the transformation shear strains are not fully annihilated by twinning in Ce-TZP, with the remaining shear strains resulting in an anisotropic plastic deformation. Theoretical examinations in Refs. 38–41 demonstrated that twinning in zirconia is influenced by the applied stress field, producing transformation shear strain which depends on the orientation of the applied stresses. In Ref. 42 it was shown that texture of the monoclinic phase exists on fracture surfaces. All these observations lead to the conclusion that the homogeneous tetragonal-to-monoclinic phase transformation produces an anisotropic plastic volume dilatation. Although a contribution of ferroelastic domain switching to the anisotropy of the plastic strains seems likely, this hypothesis is not backed by the findings of this study, because no ferroelastic domain switching was found in our experiments. Nevertheless, ferroelastic domain switching was monitored in compressive experiments,[6] which gives rise to the assumption that under tensile loads fracture occurs before the onset of domain switching.

The mechanical experiments showed a decrease of the plastic strains during unloading, which is caused by a monoclinic-to-tetragonal backtransformation. The importance of backtransformation strongly decreases with increasing grain size and nearly vanishes in CeV. From the grain size dependence and from the fact that no autocatalytic backtransformation is monitored, it can be concluded that the mechanism involved in backtransformation is similar to that of homogeneous phase transformation. As a consequence of backtransformation, it has to be acknowledged that phase content evaluations after unloading show a smaller monoclinic concentration than in-situ phase investigations.

In the experiments, no autocatalytic phase transformation could be triggered in CeI, neither by mechanical load nor by cooling. The different transformation behaviour of CeI, on the one hand, and CeII through CeV, on the other hand may be explained by several reasons. The grain size, being the main parameter characterising the different materials, should be considered the most obvious parameter responsible for the lack of autocatalytic phase transformation in CeI. It seems likely that the bimodal grain size distribution shown in Section 3.1 leads to the inhibition of autocatalytic phase transformation in regions made up by smaller grains, which have lower thermal anisotropy-induced eigenstrains, thus preventing autocatalytic transformation to have an effect on the macroscopic scale. Another explanation could be that the compressive eigenstrains produced by the large amount of homogeneous phase transformation inhibit the autocatalytic phase transformation. The effect of the porosity of 3% on the autocatalytic phase transformation remains to be investigated. A fairly different explanation might be the influence of the chemical composition of the tetragonal phase. In Section 3.1 it was shown that in CeII through CeV precipitates form during annealing, which implies that the thermal stability of the material is far from perfect. This might affect the transformation stability of the tetragonal phase. It was shown in Refs. 30,43 that a segregation of the cerium oxide may happen in Ce-TZP. In Ref. 44, a strong dependence of the stability of the tetragonal phase and of the transformation potential on the sintering parameters was found. This implies that the possibility of change in the phase composition of the matrix has to be considered. This hypothesis is underlined by the fact that the CeI specimen had a much lighter yellow colour than the materials CeII through CeV.

In Fig. 11, the critical transformation stresses of 9Ce-TZP materials found in four-point bending by various authors[8,10,14] are compared to the ones found in this

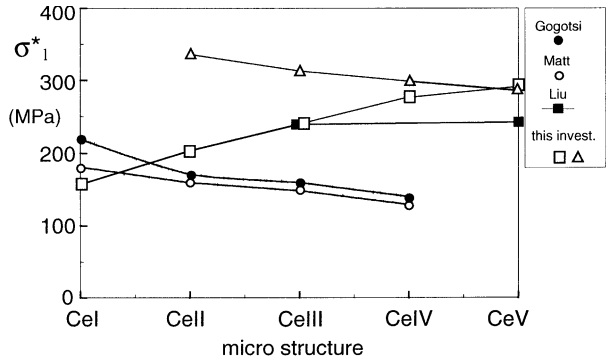

Fig. 11. Critical transformation stresses in four-point bending, as given by various authors (Gogotsi,[8] Matt,[10] Liu[14]).

investigation. Only data corresponding to materials produced with the same sintering parameters have been included. All the materials considered have been produced from nominally the same 9Ce-TZP powder by the same manufacturer, with the powder used in Refs. 8,10,14 coming from the same batch, unlike the powder used in this investigation. The data of Refs. 10,14 represent the onset of plastic deformation in the stress–strain diagram. The data of Ref. 8 were derived using acoustic emission and are comparable to σ_{AE}. A comparison of the critical stresses shows that the critical stresses of Refs. 8,10,14 are well below the ones found in our investigation Furthermore, the critical transformation stresses found in this study are above the bending strength found in Ref. 10. In Ref. 8, autocatalytic transformation and continuous plastic deformation before the onset of autocatalytic transformation was found in a material similar to CeI. In that investigation, it was assumed that this homogeneous plastic deformation is caused by ferroelastic domain switching. But the quantitative phase analysis in Section 3.5 shows that this plastic deformation is caused by the homogeneous tetragonal-to-monoclinic phase transformation. A high discrepancy also shows up when comparing the size of the transformation bands. The transformation bands observed in Ref. 10, which also occurred in CeI in that investigation, had a width of several millimetres and are, thus, nearly two orders of magnitude larger than those found in this investigation. It has to be noted that the martensitic start temperatures of this investigation are lower by 50°C than those of Ref. 10. It has to be concluded that the materials used in Refs. 8,10,14 had a fairly higher transformation potential, resulting in lower critical transformation stresses and larger transformation structures.

Because the specimens have been produced by the same sintering procedure, the composition of the two powder batches has to be considered the only differing parameter. An investigation of the particle size and distribution of both powders did not reveal any difference. When measuring the cerium oxide content of both powders using X-ray fluorescence, it was found that the cerium oxide content of the powder used in Refs. 8,10,14 was smaller by 0.2% than in the powder used in this investigation. Since zirconia with a cerium oxide content of 9 mol% are very close to the stability limit of the tetragonal phase, it has to be assumed that the differing cerium oxide content of the powders is the cause of the strong difference with the results of other authors.

5. Conclusions

For the investigation of the critical stresses initiating the tetragonal-to-monoclinic phase transformation in 9Ce-TZP zirconia, materials with five different grain sizes have been produced. Taking into account the different grain sizes, the influence of the grain size on the critical transformation stresses has been monitored.

It was found that phase transformation occurs as two different transformation types:

- A homogeneous phase transformation with a transformation strain increasing continuously with increasing applied stress. This transformation type produces the initial deviation from linear–elastic material behaviour in the stress–strain curves.
- An autocatalytic phase transformation with the autocatalytic formation of transformation bands, leading to a strongly inhomogeneous, localised distribution of the monoclinic phase. The transformation bands are oriented normal to the maximum principal stress of the applied stress field. Their location and size vary randomly. The formation of the transformation bands has been monitored by acoustic emission recording.

The grain size influences both types of phase transformation. The critical stresses of the homogeneous transformation increase with increasing grain size. The amount of homogeneous transformation strains decreases strongly with increasing grain size, leading to a strong decrease of the significance of homogeneous transformation for the overall transformation behaviour with increasing grain size. The critical stresses of the autocatalytic phase transformation show a slight decrease with increasing grain size. In the material with the smallest grain size, no autocatalytic phase transformation was found. A similar transformation behaviour was found in cooling experiments, confirming the results of the mechanical experiments.

In Raman-spectroscopic phase evaluations it was found that the autocatalytic transformation band formation leads to a local concentration of the monoclinic phase.

Strong differences compared to the critical transformation stresses investigated by other authors have been found, although the same zirconia powder had been processed using identical sintering parameters. This leads to the conclusion that the material parameters of

9Ce-TZP ceramics strongly vary among different powder batches, inferring that the production of a zirconia powder with a composition close to the stability limit of the tetragonal phase is problematic. From the microcrack-related decrease of the strength despite the high fracture toughnesses, it has to be concluded that this material is not very suitable for practical application.

Acknowledgements

This work was supported by the Deutsche Forschungsgemeinschaft (DFG).

References

1. Becher, P. F. and Swain, M. V., Grain-size-dependent transformation behaviour in polycrystalline tetragonal zirconia. *Journal of the American Ceramic Society*, 1992, **75**, 493–502.
2. Evans, A. G. and Cannon, R. M., Overview: Toughening of brittle solids by martensitic transformations. *Acta Metallurgica*, 1986, **34**, 761–800.
3. Muddle, B. C. and Hannink, R. J. H., Crystallography of the tetragonal to monoclinic transformation in MgO-partially-stabilized zirconia. *Journal of the American Ceramic Society*, 1986, **69**, 547–555.
4. Mori, T. and Tanaka, K., Average stress in matrix and average elastic energy of materials with misfitting inclusions. *Acta Metallurgica*, 1973, **21**, 571–574.
5. McMeeking, R. M. and Evans, A. G., Mechanics of transformation toughening in brittle materials. *Journal of the American Ceramic Society*, 1982, **65**, 242–247.
6. Bowman, K. J. and Chen, I.-W., Transformation textures in zirconia. *Journal of the American Ceramic Society*, 1993, **76**, 113–122.
7. Wen, S., Ma, L., Guo, J. and Yen, T., Transmission electron microscopic observation of the martensitic phase transformation in tetragonal ZrO_2. *Journal of the American Ceramic Society*, 1986, **69**, 570–572.
8. Gogotsi, G. A., Zavada, V. P. and Swain, M. V., Mechanical property characterisation of a 9 mol% Ce-TZP ceramic material — I. Flexural response. *Journal of the European Ceramic Society*, 1995, **15**, 1185–1192.
9. Hannink, R. H. J. and Swain, M. V., Metastability of the martensitic transformation in a 12 mol% ceria-zirconia alloy: I, Deformation and fracture observations. *Journal of the American Ceramic Society*, 1989, **72**, 90–98.
10. Matt, R., Statisches und Zyklisches Ermüdungsverhalten Umwandlungsverstärkter ZrO2-Werkstoffe, Dissertation, Universität Karlsruhe, IKM 016, 1996
11. Reyes-Morel, P. E., Cherng, J.-S. and Chen, I.-W., Transformation plasticity of CeO_2-stabilized tetragonal zirconia polycrystals: I, Stress assistance and autocatalysis. *Journal of the American Ceramic Society*, 1988, **71**, 343–353.
12. Sun, Q., Zhao, Z., Chen, W., Qing, X., Xu, X. and Dai, F., Experimental study of stress-induced localized transformation plastic zones in tetragonal zirconia polycrystalline ceramics. *Journal of the American Ceramic Society*, 1994, **77**, 1352–1356.
13. Gogotsi, G. A., Zavada, V. P. and Swain, M. V., Mechanical property characterization of 9 mol% Ce-TZP ceramic material — II. Fracture toughness. *Journal of the European Ceramic Society*, 1996, **16**, 545–551.
14. Grathwohl, G. and Liu, T., Crack resistance and fatigue of transforming ceramics: II, CeO_2-stabilized tetragonal ZrO_2. *Journal of the American Ceramic Society*, 1991, **74**, 3028–3034.
15. Rose, L. R. F. and Swain, M. V., Transformation zone shape in ceria-partially-stabilized zirconia,. *Acta Metallurgica*, 1988, **36**, 955–962.
16. Chen, I. W. and Reyes-Morel, P. E., Implication of transformation plasticity in ZrO_2-containing ceramics: I, Shear and dilatation effects. *Journal of the American Ceramic Society*, 1986, **69**, 181–189.
17. Bowman, K. J., Reyes-Morel, P. E. and Chen, I.-W., Reversible transformation plasticity in uniaxial tension-compression cycling of Mg-PSZ. *Material Research Society Symposium Proceedings*, vol. 78, 1987
18. Kisi, E. H., Kennedy, S. J. and Howard, C. J., Neutron diffraction observations of ferroelastic domain switching and tetragonal-to-monoclinic transformation in Ce-TZP. *Journal of the American Ceramic Society*, 1997, **80**, 621–628.
19. Marshall, D. B. and James, M. R., Reversible stress-induced martensitic transformation in ZrO_2. *Journal of the American Ceramic Society*, 1986, **69**, 215–217.
20. Liu, S.-Y. and Chen, I.-W., Plasticity-induced fatigue damage in ceria-stabilized tetragonal zirconia polycrystals. *Journal of the American Ceramic Society*, 1994, **77**, 2025–2035.
21. Prettyman, K. M., Jue, J. F., Virkar, A. V., Hubbard, C. R., Cavin, O. B. and Ferber, M. K., Hysteresity effects in 3 mol% yttria-doped zirconia (t′-Phase). *Material Science*, 1992, **27**, 4167–4174.
22. Subhash, G. and Nemat-Nasser, S., Dynamic stress-induced transformation and texture formation in uniaxial compression of zirconia ceramics. *Journal of the American Ceramic Society*, 1993, **76**, 153–156.
23. Matt, R., Grathwohl, G. and Oberacker, R., Ermüdungsverhalten umwandlungsverstärkter Y-TZP-Werkstoffe. In Materialwissenschaftliche Grundlagen, ed. G. F. Aldinger and H. Mughrabi. DGM Informationsgesellschaft, Frankfurt, 1997, pp. 583–588.
24. Liu, T., Herstellung, Degradation und Ermüdung von umwandlungsverstärkten Y-TZP(A) und Ce-TZP Werkstoffen, Thesis, University of Karlsruhe, 1990
25. Garvie, R. C. and Nicholson, P. S., Phase analysis in zirconia systems. *Journal of the American Ceramic Society*, 1972, **55**, 303–305.
26. Clarke, D. R. and Adar, F., Measurement of the crystallographically transformed zone produced by fracture in ceramics containing tetragonal zirconia. *Journal of the American Ceramic Society*, 1982, **65**, 284–288.
27. Keramidas, V. G. and White, W. B., Raman scattering study of the crystallization and phase transformation of ZrO_2. *Journal of the American Ceramic Society*, 1974, **57**, 22–24.
28. Dauskardt, R. H., Veirs, D. K. and Ritchie, R. O., Spatially resolved Raman spectroscopy study of transformed zones in magnesia-partially-stabilized zirconia. *Journal of the American Ceramic Society*, 1989, **72**, 1124–1130.
29. Lim, C. S., Finlayson, T. R., Ninio, F. and Griffiths, J. R., In-situ measurement of the stress-induced phase transformations in magnesia-stabilized zirconia using Raman spectroscopy. *Journal of the American Ceramic Society*, 1992, **75**, 1570–1573.
30. Theunissen, G. S. A. M., Winnubst, A. J. A. and Burggraaf, A. J., Effect of dopants on the sintering behaviour and stability of tetragonal zirconia ceramics. *Journal of the European Ceramic Society*, 1992, **9**, 251–263.
31. Kountouros, P. and Petzow, G., Defect chemistry. phase stability and properties of zirconia polycrystals. In Science and Technology on Zirconia, ed. S. P. S. Badwal, M. J. Bannister and R. H. J. Hannick. DGM Informationsgesellschaft, Frankfurt, 1993, pp. 30–48.
32. Fett, T. and Munz, D., Influence of time-dependent phase transformations on bending tests. *Materials Science & Engineering*, 1996, **A219**, 89–94.
33. Chen, I. W. and Reyes-Morel, P. E., Transformation plasticity and transformation toughening in Mg-PSZ and Ce-TZP. *Material Research Society Symposium Proceedings*, 1987, **78**, .

34. Chen, W., Model of transformation toughening in brittle material. *Journal of the American Ceramic Society*, 1991, **74**, 2564–2572.
35. Reyes-Morel, P. E., Cherng, J.-S. and Chen, I.-W., Transformation plasticity of CeO_2-stabilized tetragonal zirconia polycrystals: II, Pseudoelasticity and shape memory effect. *Journal of the American Ceramic Society*, 1988, **71**, 648–657.
36. Bowman, K. J., Texture from domain switching of tetragonal zirconia. *Journal of the American Ceramic Society*, 1991, **74**, 2690–2692.
37. Marshall, D. B., Strength characteristics of transformation-toughened zirconia. *Journal of the American Ceramic Society*, 1986, **69**, 173–180.
38. Lam, K. Y. and Zhang, J. M., Transformation twinning in zirconia particles. *Acta Metallurgica*, 1992, **40**, 1395–1401.
39. Lam, K. Y., Zhang, J. M. and Ong, P. P., A micromechanical model for ZrO_2-toughened ceramics. *Mechanical Materials*, 1995, **19**, 227–238.
40. Zhang, J. M. and Lam, K. Y., On transformation shear of precipitated zirconia particles. *Acta Metallurgica Materials*, 1993, **41**, 1773–1782.
41. Zhang, J. M. and Lam, K. Y., Transformation shear of precipitated ZrO_2 particles in the presence of multi-mode twinning. *International Journal of Solid Structures*, 1994, **31**, 517–532.
42. Paterson, A. W. and Stevens, R., Preferred orientation of the transformed monoclinic phase in fracture surfaces of Y-TZP ceramics. *International Journal of High Technology Ceramics*, 1986, **2**, 135–142.
43. Chaim, R., Brandon, D. G. and Heuer, A. H., A diffusional phase transformation in ZrO_2–4 wt.% Y_2O_3 induced by surface segregation. *Acta Metallurgica*, 1986, **34**, 1933–1939.
44. Heussner, K.-H. and Claussen, N., Strengthening of ceria-doped tetragonal zirconia polycrystals by reduction-induced phase transformation. *Journal of the American Ceramic Society*, 1989, **72**, 1044–1046.